Hindawi Publishing Corporation
Journal of Nanomaterials
Volume 2013, Article ID 314012, 6 pages
http://dx.doi.org/10.1155/2013/314012

Research Article

Influence of PVP on the Morphologies of Bi_2S_3 Nanostructures Synthesized by Solvothermal Method

Anukorn Phuruangrat,[1] Titipun Thongtem,[2] and Somchai Thongtem[3,4]

[1] *Department of Materials Science and Technology, Faculty of Science, Prince of Songkla University, Hat Yai, Songkhla 90112, Thailand*
[2] *Department of Chemistry, Faculty of Science, Chiang Mai University, Chiang Mai 50200, Thailand*
[3] *Department of Physics and Materials Science, Faculty of Science, Chiang Mai University, Chiang Mai 50200, Thailand*
[4] *Materials Science Research Center, Faculty of Science, Chiang Mai University, Chiang Mai 50200, Thailand*

Correspondence should be addressed to Anukorn Phuruangrat; phuruangrat@hotmail.com
and Titipun Thongtem; ttpthongtem@yahoo.com

Received 1 June 2013; Revised 5 November 2013; Accepted 27 November 2013

Academic Editor: Steve Acquah

Different morphologies of Bi_2S_3 nanostructures were synthesized by a 180°C and 12 h solvothermal reaction of solutions containing $Bi(NO_3)_3{\cdot}5H_2O$ and thioacetamide (CH_3CSNH_2) in diethylene glycol (DEG) as a solvent. The as-synthesized Bi_2S_3 products characterized by XRD, Raman spectroscopy, SEM, and TEM showed that they were well-crystallized orthorhombic Bi_2S_3 phase with morphologies of nanorod-like, sheaf-like, carnation-like, and microspherical, controlled by different contents of polyvinylpyrrolidone (PVP) in the solutions. Based on the experimental results, a growth mechanism was also proposed and discussed.

1. Introduction

Presently, nanostructured materials are very important to science and technology due to their novel optical, magnetic, and catalytic properties as compared to the corresponding bulks. They are elementary materials used for the fabrication of optoelectronic devices. Among them, the V-VI chalcogenide group with $A^V{}_2B^{VI}{}_3$ (A = As, Sb, and Bi; B = S, Se, and Te) formula has a wide variety applications in television cameras for photoconducting targets, thermoelectric devices, electronic and optoelectronic devices, and IR spectroscopy [1–8]. Bi_2S_3 is a 1.3–1.7 eV direct band gap layered semiconductor with orthorhombic crystal system and $D_{2h}{}^{16}$ or Pbnm space group, which has structure similar to Sb_2S_3 and Sb_2Se_3. It has a number of potential applications such as photovoltaic and optoelectronic, thermoelectric cooling systems, IR devices, X-ray computed tomography, photocatalysis for hydrogen evolution, and electrochemical hydrogen storage [9–11]. It is a highly anisotropic semiconductor with layered structure parallel to its growth direction and has lattice parameters of a = 11.123 Å, b = 11.282 Å, and c = 3.971 Å with pseudolayers of ribbon-like Bi_4S_6 polymers linked together by intermolecular attraction of bismuth and sulfur atoms along the [001] direction. Bond lengths within the ribbons are different due to two different types of coordination exhibited by both bismuth and sulfur. Two crystallographic independent Bi atoms belong to Bi_2S_3: Bi1 of 6-fold coordinated to three strong Bi–S bonds and three weak ones and Bi_2 of 5-fold coordinated square pyramidal sphere with three strong and two weak ones [12–15]. Morphologies of nanomaterials can play the role in the physical and chemical properties, for instances, 148 $mA{\cdot}h{\cdot}g^{-1}$ initial discharge capacity of Bi_2S_3 microflowers in lithium-ion batteries [16] and good electrochemical Li^+ insertion with 826 $mA{\cdot}h{\cdot}g^{-1}$ capacity of dandelion-like Bi_2S_3 microspheres [9]. In addition, uniform Bi_2S_3 nanodots showed higher and more stable photocatalytic activity for the degradation of persistent toxic organic pollutants under UV light irradiation than Bi_2S_3 nanorods [17]. Different morphologies and structures can play the role in energy gap (E_g) and photoluminescence (PL) of materials [1, 2, 10, 12], including their properties.

In this research, nanorods, double sheaf-like Bi_2S_3, carnation-like Bi_2S_3, and microspheres of Bi_2S_3 nanorods were sy-

nthesized by a solvothermal method in solutions containing different contents of PVP. A possible formation mechanism was proposed and discussed according to the experimental results.

2. Experimental Procedures

All chemicals were analytical grade and were used without further purification. In a typical experimental procedure, 0.0010 mol $Bi(NO_3)_3{\cdot}5H_2O$ and 0.0015 mol thioacetamide (TAA, CH_3CSNH_2) were dissolved in 80 ml of diethylene glycol (DEG) under vigorous stirring for 1 h and followed by the addition of 0.1, 0.5, and 1.0 g of polyvinylpyrrolidone (PVP) with molecular mass of 40,000 and 0.5 mL 37% HNO_3. These resulting solutions were loaded into 100 mL Teflon-lined stainless-steel autoclaves. The autoclaves were tightly closed, processed at 180°C for 12 h in an electric oven, and left cooling to room temperature naturally. At the conclusion of the process, deep gray precipitates were synthesized, filtered, washed with distilled water and absolute ethanol repeatedly to remove undesired impurities, and dried at 60°C for 4 h.

X-ray diffraction (XRD) patterns were obtained on a Philips X'Pert MPD X-ray powder diffractometer (XRD) using a Cu-K_α radiation at 45 kV and 35 mA with a scanning rate of 0.04 deg/s in the 2θ range from 15 to 60 deg. Scanning electron microscopic (SEM) analysis was conducted by a JEOL JSM-6335F electron microscope operating at 35.0 kV. Transmission electron microscopic (TEM) images, high-resolution TEM (HRTEM) images, and selected area electron diffraction (SAED) patterns were performed by a JEOL JEM-2010 transmission electron microscope at an accelerating voltage of 200 kV. A Raman spectroscopy was operated on a HORIBA Jobin Yvon T64000 spectrometer using Ar^+ laser beam of 514.5 nm wavelength, calibrated using a silicon wafer as the standard.

3. Results and Discussion

Figure 1 shows XRD patterns of Bi_2S_3 synthesized using different contents of PVP by a solvothermal method at 180°C for 12 h. Compared to the JCPDS database no. 17-0320 [18] (a = 11.1490 Å, b = 11.3040 Å, and c = 3.9810 Å), all of the diffraction patterns were interpreted as orthorhombic Bi_2S_3. No impurities of Bi_2O_3, Bi, and others were detected in these main products. The diffraction peaks were narrow and sharp, indicating that the products were of high degree of crystallinity with their atoms residing in crystalline lattice.

Figure 2 shows Raman spectra of Bi_2S_3 products over the wavelength range of 100–1800 cm^{-1}. The spectra present four peaks at 129, 251, 420, and 968 cm^{-1}. Generally, the presence of the first peak at 129 cm^{-1} can be attributed to surface optical (SO) phonon mode. The second corresponds to the vibration mode of Bi_2S_3 nanorods at 252 and 259 cm^{-1}, and Bi_2S_3 nanoribbons and hierarchical nanostructures at 250 cm^{-1}, specified as the vibration mode of Bi–S bonds. The vibration at 968 cm^{-1} was in accordance with that of Bi_2S_3 nanorods [2].

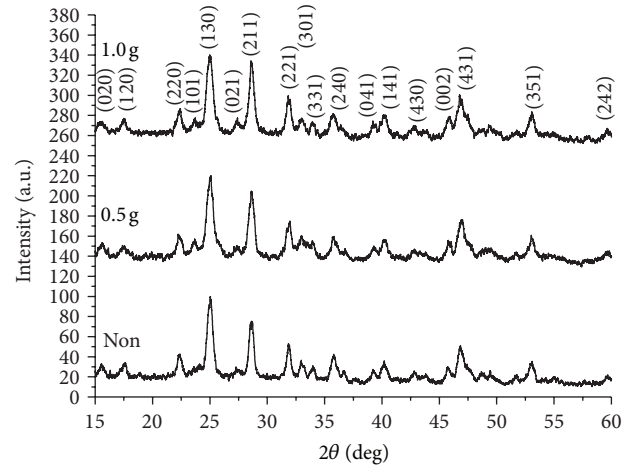

Figure 1: XRD patterns of Bi_2S_3 solvothermally synthesized in the solutions containing 0.0, 0.5, and 1.0 g PVP.

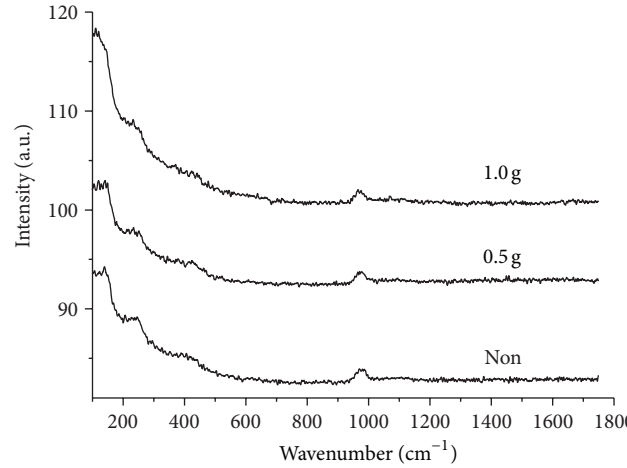

Figure 2: Raman spectra of Bi_2S_3 solvothermally synthesized in the solutions containing 0.0, 0.5, and 1.0 g PVP.

Size and structure of the products under different reaction conditions were further investigated by electron microscopy (EM). Figure 3 shows typical SEM images of the as-synthesized Bi_2S_3 products in the solutions with different PVP contents. SEM analysis reveals that Bi_2S_3 synthesized in PVP-free solution is mostly consisted of large quantity of nanorods with 0.5–2 μm in length and 50 nm in diameter. The morphologies of Bi_2S_3 products were varied in sequence by adding of different contents of PVP. The mixed morphologies of microsized double sheaf-like and carnation-like Bi_2S_3 were detected in 0.1 g PVP solution under solvothermal at 180°C for 12 h. They became uniformly and completely carnation-like Bi_2S_3 microflowers with diameter in the range of 5-6 μm in the solution containing 0.5 g PVP. High magnification of the carnation-like Bi_2S_3 nanostructure reveals the lobe of carnation-like Bi_2S_3 microsized crystals consisting of nanopetals with the shape in between rods and sheets as building blocks. By increasing the PVP content to 1.0 g, the product appeared as 3D microsphere-like Bi_2S_3. Its high

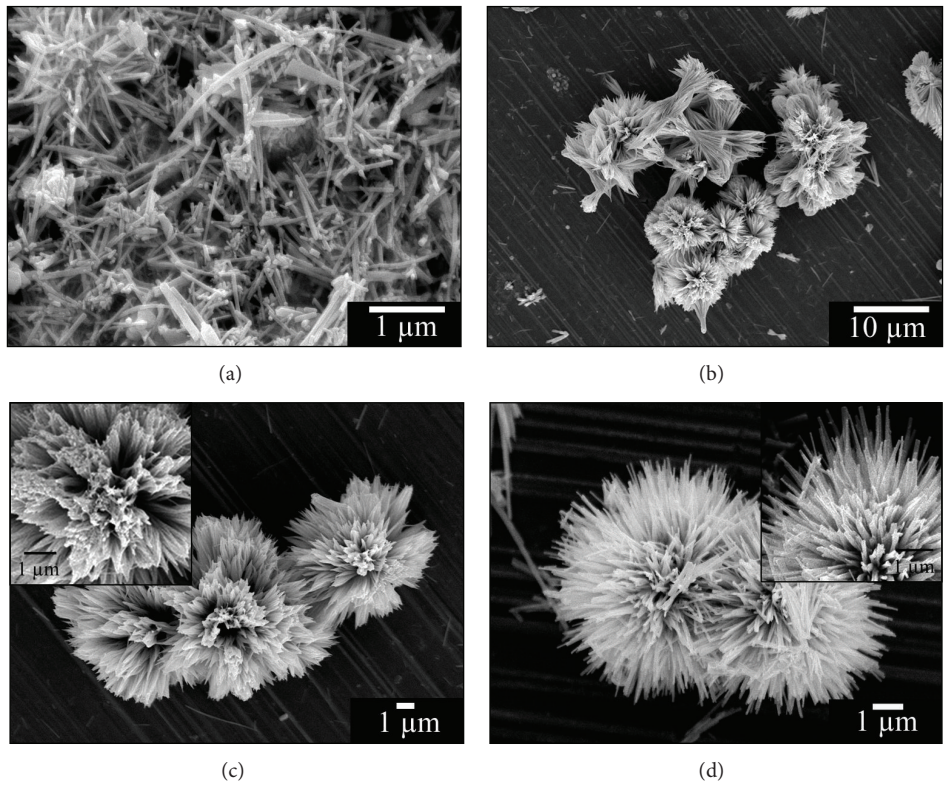

Figure 3: SEM images of Bi_2S_3 solvothermally synthesized in the solutions containing (a–d) 0, 0.1, 0.5, and 1.0 g PVP, respectively.

magnification SEM image revealed that each microsphere was composed of a number of nanorods with 3-4 μm in length and 50 nm in diameter, growing out of Bi_2S_3 core to build up 3D Bi_2S_3 microspheres. There was some difference between the carnation-like and microsphere-like products. The carnation-like flowers were composed of a number of nanopetals with the shape in between rods and sheets but the microspheres were composed of a number of nanorods with sharp tips or spears radiating from central cores. Chemical composition of the as-synthesized Bi_2S_3 microspheres was further analyzed by energy dispersive X-ray spectrometry (EDS), which revealed the presence of Bi and S in the as-synthesized Bi_2S_3 product with Bi : S atomic ratio very close to 2 : 3.

Figures 4 and 5 show TEM images of Bi_2S_3 synthesized in free-PVP, 0.1 g PVP, 0.5 g PVP, and 1.0 g PVP solutions. In PVP-free solution, the product was composed of large-scale Bi_2S_3 nanorods with an average length of 1-2 μm and diameter of 20–50 nm. Its HRTEM image was recorded on a single orthorhombic Bi_2S_3 nanorod and demonstrated that the Bi_2S_3 nanorod grew along the [001] direction. In 0.1 g PVP solution, TEM image indicates the transformation of the nanorods into the mixture of double sheaf-like and carnation-like Bi_2S_3 crystals, which were composed of a number of nanorods with the length up to a few micrometers. In 0.5 g PVP solution, the uniformly and completely carnation-like Bi_2S_3 crystals were synthesized at the same condition as above. In 1.0 g PVP solution, representative TEM image of the 3D spherical Bi_2S_3 of nanorods clearly confirmed the existence of nanostructured 3D microspheres with 4–6 μm in diameter. It was built up from uniform nanorods with diameter of about 30–50 nm and length of 3 μm. The crystalline structure of the individual Bi_2S_3 nanorods of the 3D spherical structure was characterized by HRTEM. A typical HRTEM image of an individual nanorod exhibited clear lattice fringe corresponding to the (020) plane aligning parallel to the [001] growth direction. The analysis confirmed that each nanorod was single crystal. It should be noted that the (020) planes were parallel to the individual Bi_2S_3 nanorod growth direction, indicating its preferential orientation growth along the [001] direction, due to the exceeding surface energy over other planes [2, 3, 13]. Wang et al. calculated surface energy of the (100), (010), and (001) planes of orthorhombic Bi_2S_3 structured model: 3.5878×10^{-4}, 3.4964×10^{-4}, and 4.2307×10^{-4} kJ/m^2, respectively [12]. The results supported very well with the preferential orientation growth along the *c* axis in building up of 1D nanostructured orthorhombic Bi_2S_3. For the synthesis of superparamagnetic Fe_3O_4 and $CoFe_2O_4$ with high saturation magnetization by solvothermal processing of the solution containing PVP, these products were in the shape of microspheres [19, 20].

Formation mechanism of Bi_2S_3 with different morphologies [2, 3] can be explained as follows. Bi–TAA complexes formed during stirring at room temperature. Subsequently, Bi_2S_3 was synthesized by solvothermal reaction at 180°C for 12 h. In general, HNO_3 was very important for the synthesis of 1D Bi_2S_3 nanostructure. When H^+ concentration was low, white $BiONO_3$ precipitates would be synthesized in aqueous solution by strong hydrolysis of $Bi(NO_3)_3$. Thioacetamide (CH_3CSNH_2) sulfur source gradually generated H_2S. The

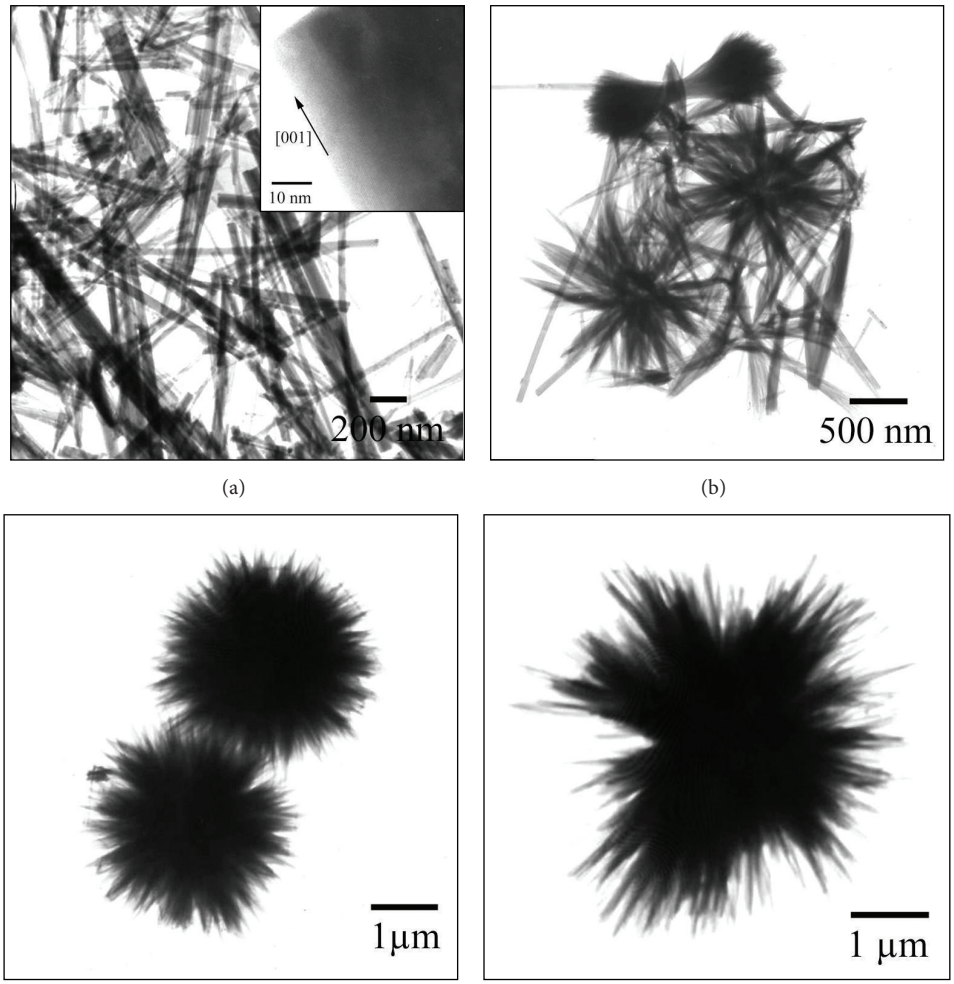

(a) (b)

(c) (d)

Figure 4: TEM and HRTEM images of Bi_2S_3 solvothermally synthesized in the solutions containing (a–d) 0, 0.1, 0.5, and 1.0 g PVP, respectively.

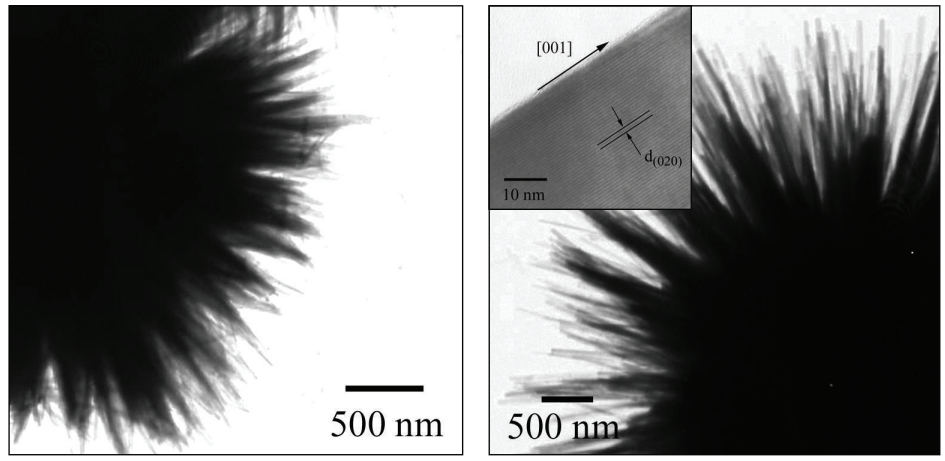

(a) (b)

Figure 5: TEM and HRTEM images of 3D microspherical Bi_2S_3 of nanorods solvothermally synthesized in the solution containing 1.0 g PVP.

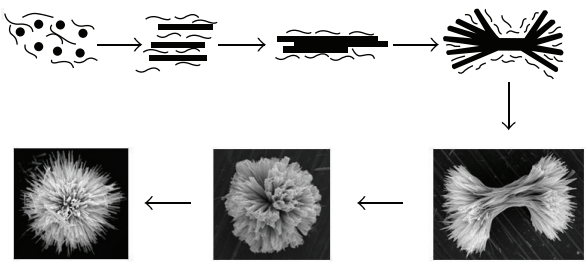

Figure 6: Schematic illustration for the formation of Bi_2S_3 nanostructures.

concentration of S^{2-} was controlled by the concentration of H^+ in the solution. In a strong acidic solution, the concentration of S^{2-} was lower, and the generation rate of Bi_2S_3 was slowed down accordingly. Thus Bi_2S_3 molecules have enough time to find their best sites to reside on crystalline seeds. Finally, one-dimensional product was formed by nucleation of molecules and growth of nuclei through the directional growth of the crystal. It should be noted that Bi_2S_3 has a lamellar structure with linked Bi_2S_3 units, which formed infinite chains parallel to the [001] direction. This anisotropic structure suggested that Bi_2S_3 has a strong tendency toward 1D growth along the [001] direction, leading to the formation of 1D nanostructure [4, 21].

In general, controlling of different shapes and sizes of materials was influenced by the presence of surfactant and polymer. The evolution of morphologies of the as-synthesized Bi_2S_3 products from nanorods in the PVP-free solution to mixed double sheaf-like and carnation-like Bi_2S_3, micro-sized carnation-like Bi_2S_3, and microspheres of nanorods in the solutions containing 0.1, 0.5, and 1.0 g of PVP surfactant under solvothermal reaction at 180°C for 12 h can be explained by a splitting mechanism, shown in Figure 6. Once Bi_2S_3 nuclei are formed just after the supersaturation process in PVP-free solution by solvothermal reaction at high temperature, Bi_2S_3 nuclei grew along the [001] direction to form nanorods, due to the strong tendency toward 1D growth along the [001] direction. In 0.1 g PVP solution, PVP macromolecules were preferentially adsorbed on the (010) planes of Bi_2S_3 nanoparticles with subsequent promoting of the growth along the [001] direction to form nanorods at a faster rate, even at the same solvothermal condition of 180°C and 12 h. PVP surfactant also promoted the splitting process at both ends of nanorods. Thus these nanorods further formed double sheaf-like structure by the splitting mechanism in combination with the growth process. Upon increasing the content of PVP from 0.1 g to 0.5 and 1.0 g at 180°C and 12 h solvothermal condition, splitting and growing of the nanorods were strengthened. Thus these products further developed into more complete carnation-like flowers and microspheres of nanospears radiating from central cores in sequence [22].

4. Conclusions

In this research, different morphologies of bismuth sulfide were synthesized in solutions containing different contents of PVP by the solvothermal reaction. The morphology evolution of Bi_2S_3 developed by 180°C and 12 h solvothermal reaction controlled by the contents of PVP in the solutions: nanorods, mixture of double sheaf-like and carnation-like Bi_2S_3, carnation-like Bi_2S_3, and microspheres of nanorods in the PVP-free, 0.1, 0.5, and 1.0 g PVP solutions, respectively. The formation of different morphologies can be explained by a splitting mechanism.

Acknowledgments

The authors wish to thank the Thailand's Office of the Higher Education Commission for providing financial support through the National Research University (NRU) Project for Chiang Mai University, and the National Nanotechnology Center (NANOTEC), National Science and Technology Development Agency, for providing financial support through the Project P-10-11345.

References

[1] W.-H. Li, "Synthesis and characterization of bismuth sulfide nanowires through microwave solvothermal technique," *Materials Letters*, vol. 62, no. 2, pp. 243–245, 2008.

[2] T. Thongtem, C. Pilapong, J. Kavinchan, A. Phuruangrat, and S. Thongtem, "Microwave-assisted hydrothermal synthesis of Bi_2S_3 nanorods in flower-shaped bundles," *Journal of Alloys and Compounds*, vol. 500, no. 2, pp. 195–199, 2010.

[3] T. Thongtem, A. Phuruangrat, S. Wannapop, and S. Thongtem, "Characterization of Bi_2S_3 with different morphologies synthesized using microwave radiation," *Materials Letters*, vol. 64, no. 2, pp. 122–124, 2010.

[4] J. Lu, Q. Han, X. Yang, L. Lu, and X. Wang, "Preparation of Bi_2S_3 nanorods via a hydrothermal approach," *Materials Letters*, vol. 61, no. 16, pp. 3425–3428, 2007.

[5] C. J. Tang, G. Z. Wang, H. Q. Wang, Y. X. Zhang, and G. H. Li, "Facile synthesis of Bi_2S_3 nanowire arrays," *Materials Letters*, vol. 62, no. 21-22, pp. 3663–3665, 2008.

[6] X. Zhu, J. Ma, Y. Wang et al., "Morphology-controlled synthesis and characterization of bismuth sulfide crystallites via a hydrothermal method," *Ceramics International*, vol. 34, no. 1, pp. 249–251, 2008.

[7] Z. Chen and M. Cao, "Synthesis, characterization, and hydrophobic properties of Bi_2S_3 hierarchical nanostructures," *Materials Research Bulletin*, vol. 46, no. 4, pp. 555–562, 2011.

[8] S.-H. Yu, J. Yang, Y.-S. Wu, Z.-H. Han, Y. Xie, and Y.-T. Qian, "Hydrothermal preparation and characterization of rod-like ultrafine powders of bismuth sulfide," *Materials Research Bulletin*, vol. 33, no. 11, pp. 1661–1666, 1998.

[9] Z. Zhang, C. Zhou, H. Lu, M. Jia, Y. Lai, and J. Li, "Facile synthesis of dandelion-like Bi_2S_3 microspheres and their electrochemical properties for lithium-ion batteries," *Materials Letters*, vol. 91, pp. 100–102, 2013.

[10] H. Kim, C. Jin, S. Park, W. I. Lee, I. J. Chin, and C. Lee, "Structure and optical properties of Bi_2S_3 and Bi_2O_3 nanostructures synthesized via thermal evaporation and thermal oxidation routes," *Chemical Engineering Journal*, vol. 215-216, pp. 151–156, 2013.

[11] A. Abdi, A. Denoyelle, N. Commenges-Bernole, and M. Trari, "Photocatalytic hydrogen evolution on new mesoporous material Bi_2S_3/Y-zeolite," *International Journal of Hydrogen Energy*, vol. 38, pp. 2070–2078, 2013.

[12] Y. Wang, J. Chen, P. Wang, L. Chen, Y.-B. Chen, and L.-M. Wu, "Syntheses, growth mechanism, and optical properties of [001] growing Bi_2S_3 nanorods," *Journal of Physical Chemistry C*, vol. 113, no. 36, pp. 16009–16014, 2009.

[13] Y. Yu and W.-T. Sun, "Uniform Bi_2S_3 nanowires: structure, growth, and field-effect transistors," *Materials Letters*, vol. 63, no. 22, pp. 1917–1920, 2009.

[14] C. An, S. Wang, and Y. Liu, "Controlled creation of self-supported patterns of radially aligned one-dimensional Bi_2S_3 nanostructures," *Materials Letters*, vol. 61, no. 11-12, pp. 2284–2287, 2007.

[15] A. Phuruangrat, T. Thongtem, and S. Thongtem, "Characterization of Bi_2S_3 nanorods and nano-structured flowers prepared by a hydrothermal method," *Materials Letters*, vol. 63, no. 17, pp. 1496–1498, 2009.

[16] H. Zhou, S. Xiong, L. Wei, B. Xi, Y. Zhu, and Y. Qian, "Acetylacetone-directed controllable synthesis of Bi_2S_3 nanostructures with tunable morphology," *Crystal Growth and Design*, vol. 9, no. 9, pp. 3862–3867, 2009.

[17] T. Wu, X. Zhou, H. Zhang, and X. Zhong, "Bi_2S_3 nanostructures: a new photocatalyst," *Nano Research*, vol. 3, no. 5, pp. 379–386, 2010.

[18] Powder Diffraction File, JCPDS-ICDD, Newtown Square, Pa, USA, 2001.

[19] H. Yuan, Y. Wang, S.-M. Zhou, and S. Lou, "Fabrication of superparamagnetic Fe_3O_4 hollow microspheres with a high saturation magnetization," *Chemical Engineering Journal*, vol. 175, no. 1, pp. 555–560, 2011.

[20] H. L. Yuan, Y. Q. Wang, S. M. Zhou et al., "Low-temperature preparation of superparamagnetic $CoFe_2O_4$ microspheres with high saturation magnetization," *Nanoscale Research Letters*, vol. 5, no. 11, pp. 1817–1821, 2010.

[21] L. Dong, Y. Chu, and W. Zhang, "A very simple and low cost route to Bi_2S_3 nanorods bundles and dandelion-like nanostructures," *Materials Letters*, vol. 62, no. 27, pp. 4269–4272, 2008.

[22] G.-Y. Chen, B. Dneg, G.-B. Cai et al., "The fractal splitting growth of Sb_2S_3 and Sb_2Se_3 hierarchical nanostructures," *Journal of Physical Chemistry C*, vol. 112, no. 3, pp. 672–679, 2008.